ORIGINAL ARTICLE

DESIGN OF A SOLAR-POWERED PADDY AND HUSK SEPARATOR MACHINE

Juan Rampengan[1*], Franklin Bawano[2], Niko Pinangkaan[3], Meidy Kawulur[4]
[1,2,3,4] Politeknik Negeri Manado, Indonesia
*Corresponding Author: juanrampengan260@gmail.com

ABSTRACT
This study designed and implemented a prototype paddy-husk separator that integrates a 200 Wp off-grid photovoltaic (PV) power system with vibrating-sieve and pneumatic separation. The mechanical assembly uses a hollow-steel frame, a perforated sieve, an eccentric drive, and a fan, while the electrical subsystem comprises a solar panel, a solar charge controller, a 12 V battery, and a 1000 W inverter. Prototype tests were reported at input loads of 10, 15, and 20 kg. The measured AC load remained at 126-132 W, which is below the inverter power rating. The pulley ratio of a 50 mm motor pulley and a 12-inch driven pulley yields a calculated sieve-shaft speed of 196.85 rpm, compared with a 214 rpm design target. Under the reported test conditions, the highest observed processing capacity was 723 kg/h at a 15 kg input load, whereas the highest reported separation efficiency (86.2%) and the lowest reported loss (1.50%) occurred at 20 kg. These results demonstrate the feasibility of integrating off-grid PV power with dual mechanical-pneumatic separation at prototype scale. However, the study does not document paddy variety, moisture content, replicate-level variability, or the full mass-balance record used to reconstruct separation efficiency and losses; therefore, field reliability, solar autonomy, and broader performance claims require further validation.

Keywords: Off-grid photovoltaic, Paddy-husk separation, Pneumatic separation, Post-harvest technology, Vibrating sieve

INTRODUCTION

Post-harvest handling remains a critical stage in the rice production chain because losses can occur during harvesting, threshing, drying, cleaning, separation, transport, and storage. In North Sulawesi, rice production continues to have strategic relevance for regional food supply, making technologies that reduce avoidable post-harvest losses practically important (Badan Pusat Statistik Provinsi Sulawesi Utara, 2025; Andriani et al., 2025). Paddy-husk separation is commonly performed through manual winnowing or mechanically assisted cleaning. Where grid electricity is limited or operational fuel costs are restrictive, smallholder-oriented equipment requires not only adequate separation performance but also an energy system that can operate independently of conventional electricity infrastructure. These conditions motivate the development of compact post-harvest machines that combine mechanical separation with locally available renewable-energy sources.

Prior studies cited in the original manuscript address important parts of this problem but generally emphasize different subsystems. Rahayu (2018) and Said et al. (2025) focused on mechanically assisted paddy sieving, while Agus (2022) developed a semi-automatic electric paddy sieve with a reported capacity of 200 kg/h but continued dependence on conventional electricity. Ulfiyah (2023) examined cyclone-based airflow separation, Sanjaya (2024) combined threshing and paddy separation, and Rusdiansyah (2023) applied solar energy to rice-threshing activities. International research on grain cleaning shows that performance is governed by the coupled effects of airflow, sieve motion, material loading, and particle characteristics. Liang et al. (2020) optimized a multi-duct rice-cleaning device using computational fluid dynamics (CFD) and experiments, whereas Xu et al. (2020) used coupled CFD-discrete element modelling to characterize gas-solid motion and predict cleaning performance. Chai et al. (2020) demonstrated that fan geometry and outlet-airflow uniformity materially influence rice-cleaning performance. A recent synthesis by Liang and Wada (2023) identifies fan design, sieve structure, airflow characterization, sensing, and adaptive control as central themes in modern combine-cleaner development. Zhao et al. (2022) further showed that airflow velocity, sieve inclination, vibration, and moisture-related particle behaviour can affect rice impurity and entrainment-loss outcomes. These findings reinforce the need to evaluate mechanical and pneumatic functions as an integrated process rather than as isolated components.

Decentralized grain-cleaning technologies can also be relevant to smallholder settings. Akatuhurira et al. (2021) developed a pedal-operated seed cleaner that combined mechanical sieving and airflow and reported substantial cleaning rates under crop-specific operating conditions. Their findings are not directly comparable with paddy-husk separation, but they illustrate the practical importance of matching separation mechanism, feed characteristics, and energy source to rural operating constraints. On the energy side, solar-powered agricultural machinery is attractive because it can reduce dependence on fossil fuel or grid access, yet PV integration introduces engineering constraints involving storage, load matching, dust, shading, temperature, and resource variability (Gorjian et al., 2021). Research on photovoltaic agricultural machinery also indicates that adoption depends on technical and economic performance attributes rather than energy source alone (Lombardi & Berni, 2021). More generally, off-grid PV-battery systems require storage and generation capacity to be matched to local resource conditions and load demand (Das & Mandal, 2022). Thus, combining a PV power system with a separator is not merely an electrical substitution; the machine load, battery, inverter, and solar resource must be considered together.

The research gap is therefore not the absence of sieves, pneumatic separation, electric motors, or solar power individually, but the limited evidence in the cited literature on integrating an off-grid PV supply with a combined vibrating-sieve and pneumatic separation mechanism in one compact paddy-husk separator and evaluating both its electrical load and prototype processing performance. Contemporary studies have advanced airflow optimization, coupled gas-solid modelling, and adaptive grain-cleaning systems, but these investigations are predominantly situated in combine-harvester architectures or powered independently of a compact off-grid PV subsystem (Liang et al., 2020; Xu et al., 2020; Liang & Wada, 2023). Conversely, renewable-energy studies emphasize solar-powered agricultural machinery and off-grid power-system sizing without directly evaluating this dual paddy-husk separation configuration (Gorjian et al., 2021; Das & Mandal, 2022). The novelty claimed here is consequently a system-level integration rather than novelty of each conventional component in isolation. This framing is intentionally conservative: the vibrating sieve, pulley-belt transmission, fan, SCC, battery, and inverter are established components, whereas the contribution lies in configuring them as one functional prototype for paddy-husk separation and reporting the resulting electrical and mechanical performance observations.

The objective of this study is to design and implement a solar-powered paddy-husk separator that combines vibrating-sieve and pneumatic separation, to characterize its mechanical transmission and electrical load, and to report prototype performance at three input-load conditions. The contribution is evaluated at prototype level through component design, calculated transmission parameters, electrical measurements, processing capacity, reported separation efficiency, and reported losses. Claims regarding long-term reliability, economic superiority, all-weather solar autonomy, and general field performance are intentionally excluded because those outcomes were not directly tested in the present study.

METHOD

Research Design and Separation Principle

This study used a design-and-build engineering approach to develop a prototype paddy-husk separator with two separation principles: mechanical vibration and pneumatic airflow. Mechanical vibration generated by an electric motor and eccentric linkage distributes the paddy-husk mixture across the perforated sieve, while the fan provides an air stream intended to displace lighter husk particles. The design rationale follows the density and aerodynamic differences between paddy and husk and the established importance of throughput, screen motion, airflow velocity, and sieve configuration in air-and-screen cleaning systems (Rahayu, 2018; Li et al., 2018; Zhao et al., 2022; Said et al., 2025). The off-grid solar PV subsystem consists of a 200 Wp panel, a maximum power point tracking (MPPT) solar charge controller (SCC), a battery, and a pure-sine-wave inverter supplying the AC loads. The estimated electrical energy generated by the panel may be expressed as $E = P \times t$, where E is electrical energy (Wh), P is panel power (W), and t is the effective solar-energy production time (h) (Fachri et al., 2015; Fuadiyah & Sudarti, 2022).

Prototype Configuration

The prototype was configured as an integrated mechanical-electrical system. The mechanical subsystem includes the structural frame, input hopper, perforated sieve, eccentric linkage, pulley-belt transmission, shafts, bearings, outlet chutes, and pneumatic fan. The electrical subsystem includes the PV panel, SCC, 12 V battery, inverter, 150 W electric motor, and 25 W AC fan. The frame uses hollow steel, while the sieve and contact surfaces use steel plate components according to the available design record. Component dimensions and specifications are reported below to support replication of the physical configuration. Unless otherwise indicated, dimensions shown in the design drawings refer to the fabricated prototype.

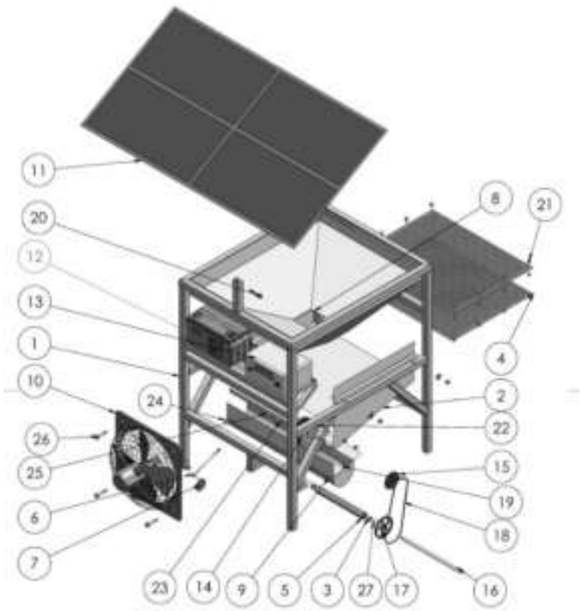

Figure 1. Prototype component plan

Table 1. Material components of the prototype

Item No.	Part	Description	Qty.
1	Structure	Hollow steel 40 × 40 × 2 mm	1
2	Sieve holder	Plate 1, Plate 2, hollow steel 20 × 25 × 1 mm	1
3	Bearing	Shaft/bearing 20 × 32, type 6804	6
4	Sieve	Steel plate, 1 mm	2
5	Shaft and bearing housing	Steel pipe	1
6	Eccentric linkage	Stainless steel, 200 mm	1
7	Coupling	Steel	1

Item No.	Part	Description	Qty.
8	Inlet hopper	Steel plate, 1 mm	1
9	Outlet chute	Steel plate, 1 mm	1
10	Exhaust fan	16/18 inch	1
11	Solar PV panel	200 Wp	1
12	Battery	12 V, 100 Ah	1
13	Inverter	1000 W pure sine wave	1
14	Electric motor	Universal Multi 1, 220 V AC	1
15	Motor pulley	A1, 2 inch, aluminum	1
16	Shaft	Steel	1
17	Driven pulley	A1, 12 inch, aluminum	1
18	V-belt	Type A-55	1
19	Nut, M12 × 1.75	Steel	9
20	Bolt, M12 × 1.75 × 70	Solar-panel lock	1
21	Bolt and nut, M10 × 1.5	Sieve lock	16 sets
22	M12 × 1.75 × 60	Motor lock	3
23	Nut, M6 × 1	Steel	2
24	Nut, M12 × 1.75	Fan lock	4
25	Bolt, M6 × 1.0 × 45	Linkage lock	1
26	Bolt, M14 × 2.0 × 70	Fan lock	4
27	Ring B27.7M-3BM1-32	Bearing lock	2

Table 2. Major tools and component specifications

No.	Component	Specification
1	Solar PV panel	200 Wp
2	Solar charge controller (SCC)	30 A, MPPT
3	Battery	12 V, 100 Ah
4	Inverter	1000 W
5	Low-voltage disconnect (LVD)	12-36 V
6	Terminal	3-branch
7	Electric motor	150 W
8	AC fan	25 W
9	Hollow steel	4 × 4 cm
10	Steel angle bar	2 × 2 cm
11	Stainless steel plate	2 mm
12	Perforated plate	Ø 10 and 8 mm
13	Bearing	Ø 32 mm
14	Eccentric linkage	20 cm
15	Pulley	12 inch
16	V-belt	Type A-55

Electrical Components

The PV panel is specified as a 200 Wp polycrystalline module with an approximately 22 V and 11 A rated output. The SCC is an MPPT controller rated at 30 A and intended for 12/24 V operation. The available battery record identifies a lithium battery rated at 12 V and 100 Ah and also lists an energy value of 768 Wh. These battery values cannot be reconciled through a simple nominal V × Ah conversion without additional manufacturer information on usable capacity or battery-management limits. For that reason, this study does not infer battery runtime or all-weather energy autonomy from the listed specification. The inverter is a 1000 W pure-sine-wave unit with 12 V DC input and 220 V AC, 50 Hz output. The 150 W AC motor drives the sieve through the eccentric linkage, and the 25 W AC fan supplies the pneumatic separation airflow.

Figure 2. Solar PV panel

Figure 3. Solar charge controller (SCC)

Figure 4. Battery

Figure 5. Inverter

Figure 6. Electric motor

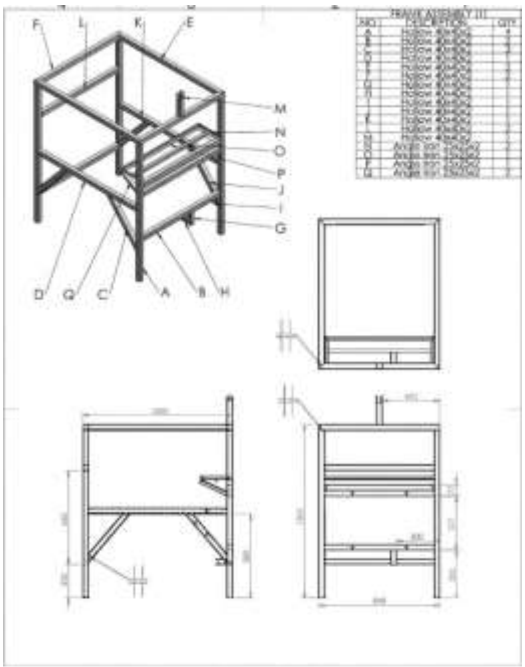

Figure 7. Prototype frame and dimensional layout

Prototype Dimensions and Geometry

The prototype geometry was selected to support gravity-assisted material flow and to provide a sufficiently rigid frame for the eccentric vibration mechanism (Shigley, 2020). The overall fabricated dimensions are approximately 100 cm in length, 84 cm in width, and 120 cm in height. The input hopper has an upper opening of 96 cm × 75.8 cm, a height of 40 cm, and a reported wall inclination of 75°. The sieve field is 75 cm long and 60 cm wide, with a reported inclination of 75.96° relative to the horizontal. The eccentric linkage length is 20 cm (200 mm), and the fan is positioned approximately 25 cm (250 mm) from the material-fall path. These geometric values are treated as design parameters of the prototype rather than as optimized settings because no multi-factor optimization experiment was reported.

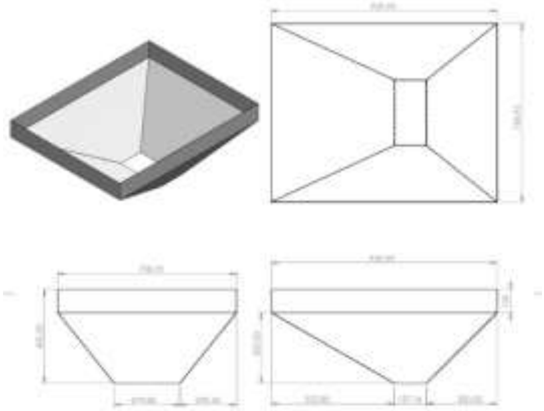

Figure 8. Input hopper design

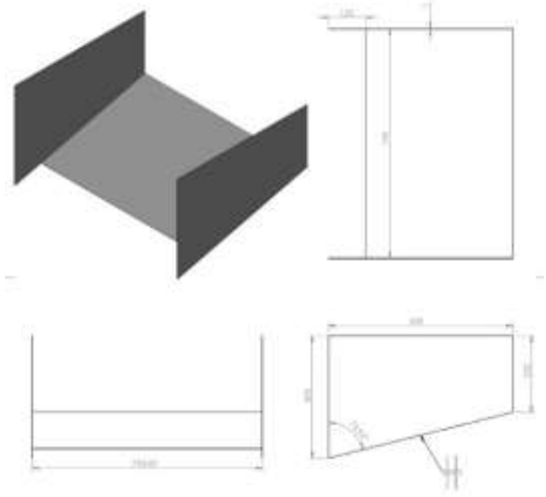

Figure 9. Sieve-unit geometry

Figure 10. Eccentric linkage

Mechanical Transmission Calculation

The electric motor transmits motion to the eccentric sieve drive through a V-belt and two pulleys (Sularso & Suga, 2002). The motor speed is N1 = 1200 rpm, the motor-pulley diameter is D1 = 50 mm, and the driven-pulley diameter is D2 = 12 inches = 304.8 mm. Using the standard pulley relationship N1D1 = N2D2, the calculated sieve-shaft speed is N2 = (1200 × 50) / 304.8 = 196.85 rpm. This is approximately 8% below the 214 rpm design target. Because the manuscript does not document tachometer measurements, 196.85 rpm is explicitly treated as a calculated transmission speed rather than an actual measured speed.

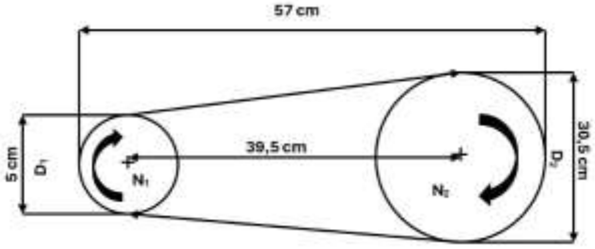

Figure 11. Pulley transmission design

The shaft center distance used in the fabricated frame was C = 395 mm. Using the common open-belt approximation $L = 2C + (\pi/2)(D1 + D2) + (D2 - D1)^2/(4C)$, the theoretical belt length is approximately 1388 mm, or 54.7 inches. This value supports selection of a commercially available Type A-55 V-belt. The calculation establishes geometric compatibility of the selected pulley and belt components; it does not substitute for direct measurements of belt slip, shaft vibration, transmitted torque, or long-term fatigue performance.

Experimental Procedure and Reporting Scope

Prototype performance was reported for three input-load conditions: 10, 15, and 20 kg. For each condition, the study record provides AC output voltage, AC load current, operational power, processing time, calculated working capacity, separation efficiency, and losses. The manuscript documentation does not specify the paddy variety, moisture content, the number of repetitions conducted at each load, the make/model or calibration status of the instruments used to measure electrical quantities and rotational speed, or replicate-level raw measurements. These parameters are therefore treated as undocumented rather than inferred. The reported results should consequently be interpreted as prototype observations under the tested conditions, not as a fully replicated performance characterization across paddy varieties or moisture levels.

Performance Indicators and Reproducibility

Working capacity was checked from the reported input mass and processing time using $C = (M/t) \times 3600$, where C is capacity (kg/h), M is input mass (kg), and t is processing time (s). This calculation reproduces the reported values; for example, 15 kg processed in 74.67 s corresponds to approximately 723 kg/h. The study record reports separation efficiency and loss percentages, but the underlying mass-balance data for clean paddy, separated husk, retained material, and lost material are not documented in the manuscript. The present revision therefore does not introduce an undocumented denominator or reconstruct those percentages from assumptions. Future replication should preserve the complete mass balance for each trial and report the equations, raw component masses, number of repetitions, and variability statistics. No human or animal participants were involved in this engineering prototype study, so human- or animal-research ethics approval and informed consent were not applicable.

RESULTS AND DISCUSSION

After fabrication and assembly, the mechanical and electrical components were integrated into a functional prototype. Figure 12 shows the assembled unit. The evaluation reported here focuses on two evidence domains: (a) electrical load during operation and the calculated transmission speed, and (b) processing performance at input loads of 10, 15, and 20 kg. Because replicate-level records and several material characteristics are not documented, the discussion distinguishes measured or reported observations from engineering interpretations and avoids treating the highest observed values as universal optima.

Figure 12. Assembled solar-powered paddy-husk separator prototype

Electrical Load and Transmission Performance

Electrical measurements reported at the AC output side of the inverter are summarized in Table 3. Across the three input-load conditions, AC output voltage was 220 V, current remained within approximately 0.57-0.60 A, and operational power remained between 126 and 132 W. The processing time increased with input load, from 64.67 s at 10 kg to 103.00 s at 20 kg.

Table 3. Electrical load measurements during prototype testing

Input load (kg)	AC output voltage (V)	AC load current (A)	Operational power (W)	Reported processing time (s)
10	220	0.57-0.59	126-130	64.67
15	220	0.58-0.60	128-132	74.67
20	220	0.58-0.60	127-131	103.00

These measurements support the limited conclusion that the observed operating load remained well below the 1000 W inverter power rating. They do not, by themselves, establish complete electrical safety, inverter efficiency, battery autonomy, thermal performance, wiring protection, or reliability under extended operation. Those broader claims would require additional protection-system documentation and measurements such as conductor current, temperature rise, inverter input power, battery state of charge, discharge depth, runtime, and energy harvested from the PV panel. This narrower interpretation directly aligns the electrical claim with the evidence actually reported.

Engineering Interpretation of the Calculated Shaft Speed

Using a motor speed of 1200 rpm, a 50 mm driving pulley, and a 12-inch driven pulley, the theoretical transmission ratio gives a calculated sieve-shaft speed of 196.85 rpm. The value is approximately 8% below the 214 rpm design target. Because no tachometer measurement is documented, the term actual rotation speed has been replaced by calculated shaft speed. A lower rotational speed may reasonably reduce excitation intensity and increase material residence time on the sieve, but effects on vibration amplitude, welded-joint durability, retention time, and separation performance were not directly measured. These effects are therefore presented as engineering interpretations, not validated causal findings. Direct measurement of shaft speed, vibration amplitude, and frequency should be included in subsequent tests to determine whether the calculated transmission ratio is maintained under load and whether belt slip materially changes operating speed.

Mechanical Processing Performance

Table 4. Reported prototype processing performance by input load

Input load (kg)	Working capacity (kg/h)	Reported separation efficiency (%)	Reported losses (%)
10	556	79.0	4.17
15	723	81.1	1.67
20	699	86.2	1.50

Table 4 shows a load-dependent trade-off between throughput and the reported separation indicators. The highest observed working capacity was 723 kg/h at 15 kg, whereas capacity decreased slightly to 699 kg/h at 20 kg. In contrast, the highest reported separation efficiency (86.2%) and the lowest reported losses (1.50%) occurred at 20 kg. The working-capacity values are consistent with the reported processing times through $C = (M/t) \times 3600$. The results therefore support a descriptive conclusion that the tested prototype processed material fastest at the 15 kg condition, while the 20 kg condition produced the most favorable reported separation and loss values. Because variability statistics and replicate-level observations are unavailable, the term optimal is not used; the results are described as the highest or lowest observed values under the three tested conditions.

Benchmarking Against Related Grain-Cleaning Technologies

The present results should be interpreted against prior devices with caution because machine architecture, crop material, feed rate, moisture, sieve geometry, and performance definitions differ across studies. Agus (2022) reported a 200 kg/h semi-automatic paddy sieve using grid-supplied electricity, whereas the present prototype reached a higher observed throughput under its own test conditions while using an off-grid PV-battery-inverter supply. Akatuhurira et al. (2021) reported cleaning rates up to 576.5 kg/h and maize cleaning efficiency above 95% for a pedal-operated multi-seed cleaner; those results demonstrate the potential of decentralized cleaning devices but are not directly comparable with paddy-husk separation because the crops, mechanisms, and definitions of efficiency differ. In high-capacity rice-cleaning research, Liang et al. (2020) demonstrated that working load and airflow distribution materially influence sieve loss and impurity, while Li et al. (2018) showed that increasing throughput reduces airflow velocity above and below a vibrating screen and can degrade cleaning performance. Chai et al. (2020) showed that improved fan geometry can increase the uniformity of outlet airflow, and Xu et al. (2020) developed CFD-DEM-based relationships between particle dispersion and cleaning performance. Zhao et al. (2022) likewise confirmed the coupled influence of airflow, sieve inclination, vibration, and rice moisture on cleaning outcomes. Bieniek et al. (2021), Kharchenko et al. (2021), and Kolankowska et al. (2022) further demonstrate the importance of aerodynamic conditions in grain separation. Therefore, the current results should not be presented as evidence of universal superiority over prior machines. The stronger scholarly contribution is the integrated PV-powered prototype and the empirical description of its own performance envelope.

Design Integration and Operating-Condition Interpretation

The combined vibrating-sieve and pneumatic configuration should be understood as a coupled separation system rather than as two independent devices. The vibrating sieve redistributes the material layer, changes the residence time of particles on the screen, and repeatedly exposes lighter fractions to the air stream. In pneumatic grain cleaning, separation quality depends not only on nominal fan power but also on airflow distribution, layer thickness, particle density, size, shape, and the degree to which the feed is stratified before or during exposure to the air stream (Kharchenko et al., 2021; Kolankowska et al., 2022). Stepanenko et al. (2022) further showed theoretically that non-uniform air-velocity fields can alter grain trajectories in pneumatic separation channels, reinforcing the importance of airflow distribution rather than fan rating alone. This interaction provides a plausible explanation for why the three input-load conditions did not produce the same ranking for throughput and separation indicators. A moderate load can favor faster passage through the machine, whereas a larger load may alter bed formation and exposure to airflow in ways that improve the recorded separation percentage but extend processing time. Because airflow velocity, bed thickness, moisture content, and particle trajectories were not measured in the present study, this explanation remains interpretive and should not be treated as a verified mechanism.

The same caution applies to the calculated sieve-shaft speed. Its proximity to operating speeds used in other separator systems may be technically reasonable, but direct equivalence cannot be claimed without measuring vibration amplitude, frequency, and actual rotational speed under load. Future experiments should therefore treat input load, sieve inclination, perforation size, fan speed or airflow rate, and paddy moisture as controlled factors rather than changing one condition without documenting the others. A factorial or response-surface design with repeated trials would allow the capacity-separation trade-off to be quantified with uncertainty and would provide stronger evidence for selecting a genuinely optimal operating point. Such a design would also allow the interaction between mechanical vibration and pneumatic airflow to be evaluated rather than inferred from only three load conditions.

Practical Significance, Transferability, and Limitations

The prototype is conceptually relevant to small- and medium-scale post-harvest operations where access to grid electricity is limited, because the measured operating load is compatible with the installed inverter and the energy source is configured as an off-grid PV system. Nevertheless, practical transferability remains provisional. The study did not quantify battery runtime, daily solar-energy balance, inverter efficiency, irradiance sensitivity, component maintenance requirements, replacement-part availability, economic cost, grain-variety effects, or performance across different moisture contents. Solar-powered agricultural machinery is sensitive to storage capacity, power matching, and environmental operating conditions (Gorjian et al., 2021), while adoption of photovoltaic agricultural machinery also depends on technical and economic attributes that were not measured in this prototype study (Lombardi & Berni, 2021). Off-grid energy-system studies likewise show that generation and battery sizing must be assessed against resource variability and load requirements rather than inferred from nominal component ratings alone (Das & Mandal, 2022). Pneumatic grain separation is simultaneously sensitive to airflow and particle characteristics (Kharchenko et al., 2021; Kolankowska et al., 2022). These limitations are important for rural deployment because a prototype that operates successfully during short tests may still face constraints during prolonged use, cloudy conditions, high dust exposure, or changes in crop moisture.

Future validation should use repeated trials and report the number of repetitions, mean values, standard deviations or confidence intervals, and the exact material characteristics for each trial. Paddy variety and moisture content should be documented because both can change particle behavior and separation response. Actual shaft speed should be measured with a tachometer, airflow should be measured at defined locations, and a complete mass balance should record input paddy-husk mixture, recovered paddy, separated husk, retained material, and losses. Long-duration tests should evaluate bearings, belt wear, frame and weld integrity, motor temperature, battery cycling, and inverter performance. PV tests should document irradiance, panel voltage/current, charge state, and runtime. If the device is later promoted on economic grounds, acquisition, maintenance, replacement, and energy costs should also be measured rather than inferred.

Transparency Statement

The numerical performance data available for this study are summarized in Tables 3 and 4. Replicate-level raw data, the complete mass-balance worksheet for separation efficiency and losses, detailed measurement-instrument specifications, and long-duration field-test records were not documented in the manuscript materials. Accordingly, the revised paper does not create or infer missing observations. The separation-efficiency and loss percentages are reported as recorded values, while working capacity is independently reproducible from the reported mass and processing time. This distinction improves transparency and defines the evidence boundary for the conclusions.

CONCLUSION

This study produced a prototype solar-powered paddy-husk separator that integrates a 200 Wp off-grid PV subsystem with vibrating-sieve and pneumatic separation. During the reported tests, operational power remained between 126 and 132 W, demonstrating that the observed AC load was within the 1000 W inverter rating. The pulley configuration of a 50 mm motor pulley and a 12-inch driven pulley yields a calculated sieve-shaft speed of 196.85 rpm, approximately 8% below the 214 rpm design target. Among the three tested input loads, the highest observed processing capacity was 723 kg/h at 15 kg, while the highest reported separation efficiency (86.2%) and lowest reported loss (1.50%) occurred at 20 kg, indicating a throughput-separation trade-off under the reported conditions. The principal contribution is the prototype-level integration of off-grid PV power with dual vibrating and pneumatic paddy-husk separation rather than the introduction of a novel individual component. Because paddy characteristics, replicate-level variability, complete mass-balance records, battery runtime, actual shaft-speed measurement, and long-term durability were not documented, claims of optimality, full energy independence, long-term reliability, and broad field generalizability remain to be validated through repeated and extended field testing.

REFERENCES

Agus, M. (2022). Rancang bangun mesin pengayak padi semi otomatis kapasitas 200 kg/jam menggunakan motor listrik. *INOTEK*, 6(2), 328-332.

Akatuhurira, W., Tumutegyereize, P., Oluk, I., Baidhe, E., Kigozi, J., Mayanja, I., & Kivumbi, H. B. (2021). Development and performance evaluation of a pedal operated seed cleaner (POS-Cleaner). *SN Applied Sciences*, 3, 675. https://doi.org/10.1007/s42452-021-04612-6

Andriani, L., Kusrini, N., & Maswadi, M. (2025). Losses in each stage of rice harvest and postharvest. *Jurnal Ilmu Pertanian Indonesia*, 30(1), 85-98.

Anugrah, A. (2023). Perancangan sistem kelistrikan pada mesin perontok padi bertenaga listrik. *Rang Teknik Journal*, 6(2), 154-166.

Badan Pusat Statistik Provinsi Sulawesi Utara. (2025). *Luas panen dan produksi padi Provinsi Sulawesi Utara 2024*. BPS Provinsi Sulawesi Utara.

Bieniek, J., Komarnicki, P., & Detyna, J. (2021). Innovative aerodynamic grain separation system for plant harvesting in sloped areas: Problems, research and optimization of parameters. *Archives of Civil and Mechanical Engineering*, 21, 27. https://doi.org/10.1007/s43452-021-00174-x

Chai, X., Xu, L., Sun, Y., Liang, Z., Lu, E., & Li, Y. (2020). Development of a cleaning fan for a rice combine harvester using computational fluid dynamics and response surface methodology to optimise outlet airflow distribution. *Biosystems Engineering*, 192, 232-244. https://doi.org/10.1016/j.biosystemseng.2019.12.016

Das, M., & Mandal, R. (2022). The effect of photovoltaic energy penetration on a photovoltaic-biomass-lithium-ion off-grid system and system optimization for the agro-climatic zones of West Bengal. *Sustainable Energy Technologies and Assessments*, 53, 102593. https://doi.org/10.1016/j.seta.2022.102593

Fachri, M. R., Sara, I. D., & Syahrizal. (2015). Analisis sistem pembangkit listrik tenaga surya off-grid sebagai sumber energi alternatif. *Jurnal Rekayasa Elektrika*, 11(5), 167-173.

Fuadiyah, T., & Sudarti, S. (2022). Potensi pemanfaatan sel surya untuk mendukung energi di bidang pertanian. *JTPG*, 7(2), 75-79.

Gorjian, S., Ebadi, H., Trommsdorff, M., Sharon, H., Demant, M., & Schindele, S. (2021). The advent of modern solar-powered electric agricultural machinery: A solution for sustainable farm operations. *Journal of Cleaner Production*, 292, 126030. https://doi.org/10.1016/j.jclepro.2021.126030

Kharchenko, S., Borshch, Y., Kovalyshyn, S., Piven, M., Abduev, M., Miernik, A., Popardowski, E., & Kiełbasa, P. (2021). Modeling of aerodynamic separation of preliminarily stratified grain mixture in vertical pneumatic separation duct. *Applied Sciences*, 11(10), 4383. https://doi.org/10.3390/app11104383

Kolankowska, E., Choszcz, D. J., Markowski, P., Reszczyński, P. S., & Lipiński, A. J. (2022). The process of separating buckwheat and wheat grain in a pneumatic cone separator in the context of sustainable agriculture. *Processes*, 10(1), 59. https://doi.org/10.3390/pr10010059

Li, Y., Xu, L., Zhou, Y., Li, B., Liang, Z., & Li, Y. (2018). Effects of throughput and operating parameters on cleaning performance in air-and-screen cleaning unit: A computational and experimental study. *Computers and Electronics in Agriculture*, 152, 141-148. https://doi.org/10.1016/j.compag.2018.07.019

Liang, Z., Xu, L., De Baerdemaeker, J., Li, Y., & Saeys, W. (2020). Optimisation of a multi-duct cleaning device for rice combine harvesters utilising CFD and experiments. *Biosystems Engineering*, 190, 25-40. https://doi.org/10.1016/j.biosystemseng.2019.11.016

Liang, Z., & Wada, M. E. (2023). Development of cleaning systems for combine harvesters: A review. *Biosystems Engineering*, 236, 79-102. https://doi.org/10.1016/j.biosystemseng.2023.10.018

Lombardi, G. V., & Berni, R. (2021). Renewable energy in agriculture: Farmers' willingness-to-pay for a photovoltaic electric farm tractor. *Journal of Cleaner Production*, 313, 127520. https://doi.org/10.1016/j.jclepro.2021.127520

Mainil, R. I., Taufik, M., & Aziz, A. (2021). Unjuk kerja mesin pemisah gabah dan sekam tipe pneumatic transport berdasarkan variasi kecepatan udara. *Jurnal Teknologi Rekayasa Teknik Mesin (REKAYASA)*, 14(2), 88-94.

Rahayu, D. P. (2018). Perancangan desain alat pengayak padi. *Seminar Nasional Teknologi dan Rekayasa (SENTRA)*.

Rusdiansyah, R. (2023). Pemanfaatan mesin perontok padi berbasis energi surya kepada kelompok tani di Kabupaten Paser. *Jurnal Pengabdian Kolaborasi dan Inovasi IPTEKS*, 1(6).

Said, A. P., Haluti, S., Staddal, I., & Mustofa, M. (2025). Rancang bangun mesin pengayak gabah padi. *Jurnal Teknologi Pertanian Gorontalo (JTPG)*, 10(1), 13-18. https://doi.org/10.30869/jtpg.v10i1.1458

Sanjaya, R. (2024). *Rancang bangun mesin perontok padi dengan pemisah gabah* [Final project]. Politeknik.

Shigley, J. E. (2020). *Mechanical engineering design* (11th ed.). McGraw-Hill.

Stepanenko, S., Kotov, B., Kuzmych, A., Shvydia, V., Kalinichenko, R., Kharchenko, S., Shchur, T., Kocira, S., Kwaśniewski, D., & Dziki, D. (2022). To the theory of grain motion in an uneven air flow in a vertical pneumatic separation channel with an annular cross section. *Processes*, 10(10), 1929. https://doi.org/10.3390/pr10101929

Sularso, & Suga, K. (2002). *Dasar perencanaan dan pemilihan elemen mesin*. PT Pradnya Paramita.

Ulfiyah, L. (2023). Implementasi alat pemisah gabah padi menggunakan sistem cyclone sebagai upaya meningkatkan efektivitas pekerjaan buruh tani. *SWGT*, 8(1), 1080-1092.

Xu, L., Li, Y., Chai, X., Wang, G., Liang, Z., Li, Y., & Li, B. (2020). Numerical simulation of gas-solid two-phase flow to predict the cleaning performance of rice combine harvesters. *Biosystems Engineering*, 190, 11-24. https://doi.org/10.1016/j.biosystemseng.2019.11.014

Zhao, L., Chen, L., Yuan, F., & Wang, L. (2022). Simulation study of rice cleaning based on DEM-CFD coupling method. *Processes*, 10(2), 281. https://doi.org/10.3390/pr10020281